CHAPTER 1

NONLINEAR SIMULATION OF DRIFT WAVE TURBULENCE

Ryusuke Numata, Rowena Ball, Robert L. Dewar
Department of Theoretical Physics, Research School of Physical Sciences and Engineering, The Australian National University, Canberra ACT 0200, Australia
E-mail: ryusuke.numata@anu.edu.au

In a two-dimensional version of the modified Hasegawa-Wakatani (HW) model, which describes electrostatic resistive drift wave turbulence, the resistive coupling between vorticity and density does not act on the zonal components ($k_y = 0$). It is therefore necessary to modify the HW model to treat the zonal components properly. The modified equations are solved numerically, and visualization and analysis of the solutions show generation of stable zonal flows, through conversion of turbulent kinetic energy, and the consequent turbulence and transport suppression. It is demonstrated by comparison that the modification is essential for generation of zonal flows.

1. Introduction

In quasi two-dimensional (2D) plasma and fluid flows the energy flux from small scale turbulent modes toward lower wavenumber modes can dominate the classical Kolmogorov cascade to dissipative scales, with the result that energy can accumulate in large scale coherent structures. Zonal flows in planetary atmospheres and in magnetically confined fusion plasmas are well-known examples of such coherent structures. Quasi two-dimensional fluid systems in which turbulent activities and coherent structures interact can undergo a spontaneous transition to a turbulence-suppressed regime. In plasmas such transitions dramatically enhance the confinement and are known as L–H or confinement transitions. From theoretical and experimental works the importance of shear or zonal flows for suppression of cross-field transport and confinement improvement is now widely appreciated.

Several low-dimensional dynamical models, comprised of a small num-

ber of coupled ordinary differential equations, have been proposed to describe and predict the L–H transition[1,2,3]. Ball *et al.* have analyzed a three-variable model using bifurcation and singularity theories[3]. The model is based on the reduced resistive magnetohydrodynamic equations with the electrostatic approximation, and describes the pressure-gradient-driven turbulence–shear flow energetics. This approach using low-dimensional modeling greatly simplifies the problem, and when validated against simulated or real experimental data, will provide an economical tool to predict transitions over the parameter space.

In this work we report the results of numerical simulations that both complement the low-dimensional modeling results and raise some interesting issues in their own right. We focus on a model for electrostatic resistive drift wave turbulence, the Hasegawa-Wakatani (HW) model[4], and solve the equations by direct numerical simulation in 2D slab geometry. The HW model has been widely used to investigate anomalous edge transport due to collisional drift waves[5]. Moreover, self-organization of a shear flow has been shown by numerical simulation of the HW model in cylindrical geometry[6]. Thus we consider the HW model is a good starting point for studying self-consistent turbulence–shear flow interactions, even though it does not describe physics that can be important in specific situations, such as magnetic curvature, magnetic shear, and electromagnetic effect.

2. Modified Hasegawa-Wakatani Model

The physical setting of the HW model may be considered as the edge region of a tokamak plasma of nonuniform density $n_0 = n_0(x)$ and in a constant equilibrium magnetic field $\boldsymbol{B} = B_0 \nabla z$. Following the drift wave ordering[7], the density $n = n_0 + n_1$ and the electrostatic potential φ perpendicular to the magnetic field are governed by the continuity equation for ions or electrons and the ion vorticity equation,

$$\frac{\mathrm{d}}{\mathrm{d}t} n = \frac{1}{e} \frac{\partial}{\partial z} j_z, \tag{1}$$

$$\frac{mn}{B_0} \frac{\mathrm{d}}{\mathrm{d}t} \nabla_\perp^2 \varphi = B_0 \frac{\partial}{\partial z} j_z, \tag{2}$$

where $\nabla_\perp = (\partial/\partial x, \partial/\partial y)^T$, $\mathrm{d}/\mathrm{d}t = \partial/\partial t + \boldsymbol{V}_E \cdot \nabla_\perp$ is the $\boldsymbol{E} \times \boldsymbol{B}$ convective derivative ($\boldsymbol{V}_E \equiv -\nabla_\perp \varphi \times \nabla z / B_0$, $\boldsymbol{E} = -\nabla_\perp \varphi$), m is the ion mass, j_z is the current density in the direction of the magnetic field. The continuity equation (1) can refer to ions and electrons because $\nabla \cdot \boldsymbol{j} = 0$ under the quasineutral condition, and (2) holds because the current density is

divergence-free. Since the ion inertia is negligible in the parallel direction (z), the parallel current is determined by the Ohm's law,

$$\boldsymbol{E} + \frac{1}{en}\nabla p_{\rm e} = \eta \boldsymbol{j}. \tag{3}$$

If the parallel heat conductivity is sufficiently large, the electrons may be treated as isothermal: $p_{\rm e} = nT_{\rm e}$ (p is the pressure, T is the temperature, and subscript e refers to electrons.) This gives the parallel current as

$$j_z = -\frac{1}{\eta}\frac{\partial}{\partial z}\left(\varphi - \frac{T_{\rm e}}{e}\ln n\right). \tag{4}$$

If we eliminate j_z from (1), (2) and normalize variables as

$$x/\rho_{\rm s} \to x, \quad \omega_{\rm ci} t \to t, \quad e\varphi/T_{\rm e} \to \varphi, \quad n_1/n_0 \to n, \tag{5}$$

where $\omega_{\rm ci} \equiv eB_0/m$ is the ion cyclotron frequency, and $\rho_{\rm s} \equiv \sqrt{T_{\rm e}/m}\omega_{\rm ci}^{-1}$ is the ion sound Larmor radius, we finally obtain the resistive drift wave equations known as the Hasegawa-Wakatani (HW) model[4],

$$\frac{\partial}{\partial t}\zeta + \{\varphi, \zeta\} = \alpha(\varphi - n) - D_\zeta \nabla^4 \zeta, \tag{6}$$

$$\frac{\partial}{\partial t} n + \{\varphi, n\} = \alpha(\varphi - n) - \kappa\frac{\partial \varphi}{\partial y} - D_n \nabla^4 n, \tag{7}$$

where $\{a, b\} \equiv (\partial a/\partial x)(\partial b/\partial y) - (\partial a/\partial y)(\partial b/\partial x)$ is the Poisson bracket, $\nabla^2 = \partial^2/\partial x^2 + \partial^2/\partial y^2$ is the 2D Laplacian, $\zeta \equiv \nabla^2\varphi$ is the vorticity. We omit $\perp$, and use ∇ for the 2D derivative. The dissipative terms with constant coefficients D_ζ and D_n have been included as adjuncts without derivation, for numerical stability. The background density is assumed to have an unchanging exponential profile: $\kappa \equiv -(\partial/\partial x)\ln n_0$. $\alpha \equiv -T_{\rm e}/(\eta n_0 \omega_{\rm ci} e^2)\partial^2/\partial z^2$ is the adiabaticity operator describing the parallel electron response. In a 2D setting the coupling term operator α becomes a constant coefficient, or parameter, by the replacement $\partial/\partial z \to {\rm i}k_z$. This resistive coupling term must be treated carefully in a 2D model because zonal components of fluctuations (the $k_y = k_z = 0$ modes) do not contribute to the parallel current[8]. Recalling that the tokamak edge turbulence is considered here, $k_y = 0$ should always coincide with $k_z = 0$ because any potential fluctuation on the flux surface is neutralized by parallel electron motion. Let us define zonal and non-zonal components of a variable f as

$$\text{zonal: } \langle f \rangle = \frac{1}{L_y}\int f {\rm d}y, \quad \text{non-zonal: } \tilde{f} = f - \langle f \rangle, \tag{8}$$

where L_y is the periodic length in y, and remove the contribution by the zonal components in the resistive coupling term in (6) and (7). By subtracting the zonal components from the resistive coupling term $\alpha(\varphi - n) \to \alpha(\tilde{\varphi} - \tilde{n})$, we end up with the modified HW (MHW) equations,

$$\frac{\partial}{\partial t}\zeta + \{\varphi, \zeta\} = \alpha(\tilde{\varphi} - \tilde{n}) - D_\zeta \nabla^4 \zeta, \tag{9}$$

$$\frac{\partial}{\partial t}n + \{\varphi, n\} = \alpha(\tilde{\varphi} - \tilde{n}) - \kappa\frac{\partial \varphi}{\partial y} - D_n \nabla^4 n. \tag{10}$$

The evolution of the zonal components can be extracted from (9) and (10) by averaging in the y direction:

$$\frac{\partial}{\partial t}\langle f \rangle + \frac{\partial}{\partial x}\langle f v_x \rangle = D\nabla^2 \langle f \rangle, \quad v_x \equiv -\frac{\partial \tilde{\varphi}}{\partial y}, \tag{11}$$

where f stands for ζ and n, and D stands for the corresponding dissipation coefficients.

The HW model spans two limits with respect to the adiabaticity parameter. In the adiabatic limit $\alpha \to \infty$ (collisionless plasma), the non-zonal component of electron density obeys the Boltzmann relation $\tilde{n} = n_0(x)\exp(\tilde{\varphi})$, and the equations are reduced to the Hasegawa-Mima equation[7]. In the hydrodynamic limit $\alpha \to 0$ and the equations are decoupled. Vorticity is determined by the 2D Navier-Stokes (NS) equation, and the density fluctuation is passively advected by the flow obtained from the NS equation.

In the ideal limit ($\alpha = \infty$, $D_\zeta = D_n = 0$) the modified HW system has two dynamical invariants, the energy E and the potential enstrophy W,

$$E = \frac{1}{2}\int (n^2 + |\nabla\varphi|^2)\mathrm{d}\boldsymbol{x}, \quad W = \frac{1}{2}\int (n - \zeta)^2 \mathrm{d}\boldsymbol{x}, \tag{12}$$

where $\mathrm{d}\boldsymbol{x} = \mathrm{d}x\mathrm{d}y$, which constrain the fluid motion. According to Kraichnan's theory of 2D turbulence[9], the net flux of enstrophy is downscale while that of energy is upscale. This inverse energy cascade is behind the development of large scale, stable coherent structures in a HW flow.

Conservation laws are given by

$$\frac{\mathrm{d}E}{\mathrm{d}t} = \Gamma_n - \Gamma_\alpha - D_E, \quad \frac{\mathrm{d}W}{\mathrm{d}t} = \Gamma_n - D_W. \tag{13}$$

Fluxes and dissipations are given by

$$\Gamma_n = -\kappa \int \tilde{n} \frac{\partial \tilde{\varphi}}{\partial y} \mathrm{d}\boldsymbol{x}, \tag{14}$$

$$\Gamma_\alpha = \alpha \int (\tilde{n} - \tilde{\varphi})^2 \mathrm{d}\boldsymbol{x}, \tag{15}$$

$$D_E = \int [D_n (\nabla^2 n)^2 + D_\zeta |\nabla \zeta|^2] \mathrm{d}\boldsymbol{x}, \tag{16}$$

$$D_W = \int [D_n (\nabla^2 n)^2 + D_\zeta (\nabla^2 \zeta)^2 - (D_n + D_\zeta) \nabla^2 n \nabla^2 \zeta] \mathrm{d}\boldsymbol{x}. \tag{17}$$

These quantities constitute sources and sinks. As will be seen in the simulation results, they are mostly positive (Γ_α and D_E are positive definite), thus only Γ_n can act as a source. The energy absorbed from the background supplies the turbulent fluctuations through the drift wave instability.

Note that the same conservation laws hold for the unmodified original HW (OHW) model except that Γ_α is defined by both zonal and non-zonal components; $\Gamma_\alpha^{\mathrm{OHW}} \equiv \alpha \int (n - \varphi)^2 \mathrm{d}\boldsymbol{x}$. In the OHW model, the zonal modes as well as the non-zonal modes suffer the resistive dissipation.

2.1. *Linear Stability Analysis*

Since the zonal modes have linearly decaying solutions, we only consider the form $e^{\mathrm{i}(k_x x + k_y y - \omega t)}$ ($k_y \neq 0$). Linearization of the equations (9) and (10) yields the dispersion relation,

$$\omega^2 + \mathrm{i}\omega(b + (1 + P_r^{-1}) k^4 D_\zeta) - \mathrm{i} b \omega_* - \alpha k^2 (k^2 + P_r^{-1}) D_\zeta - k^8 P_r^{-1} D_\zeta^2 = 0, \tag{18}$$

where we defined $k^2 = k_x^2 + k_y^2$, $b \equiv \alpha(1 + k^2)/k^2$, the drift frequency $\omega_* \equiv k_y \kappa / (1 + k^2)$, and the Prandtl number $P_r \equiv D_\zeta / D_n$. Solutions to the dispersion relation (18) are given by

$$\Re(\omega) = \pm \frac{1}{2} (\sigma^2 + 16 b^2 \omega_*^2)^{\frac{1}{4}} \cos \frac{\theta}{2}, \tag{19}$$

$$\Im(\omega) = -\frac{1}{2} \left[b + (1 + P_r^{-1}) k^4 D_\zeta \mp (\sigma^2 + 16 b^2 \omega_*^2)^{\frac{1}{4}} \sin \frac{\theta}{2} \right], \tag{20}$$

$\sigma = 4\alpha k^2 (k^2 + P_r^{-1}) D_\zeta + 4 k^8 P_r^{-1} D_\zeta^2 - (b + (1 + P_r^{-1}) k^4 D_\zeta)^2$, $\tan\theta = 4 b \omega_* / \sigma$. In the limit where $D_\zeta = D_n = 0$, it is readily proved that one of the growth rate $\gamma \equiv \Im(\omega)$ is positive if $b\omega_*$ is finite, thus unstable. However, there exists a range of D_ζ where the drift wave instability is suppressed. The stability threshold is given by

$$\left(b + (1 + P_r^{-1}) k^4 D_\zeta \right)^4 \geq (\sigma^2 + 16 b^2 \omega_*^2) \sin^4 \frac{\theta}{2}, \tag{21}$$

and is depicted in Fig. 1. The left panel shows the stability boundary in $D_\zeta - \kappa$ plane. If we enhance the drive by increasing κ, the system becomes unstable. However, the instability is stabilized by increasing the dissipation. The stability threshold in $k_x - k_y$ plane is shown in the right panel. We see that in a highly driven-dissipative system only low wavenumber modes are unstable. The stability boundary in parameter space is a region where interesting dynamics are expected to occur, such as bifurcations or sudden changes to a suppressed (or enhanced) turbulence regime.

Figure 2 shows the dispersion relation for cases where $D_\zeta = D_n = 0$. To provide a test of the simulation code, we plot growth rates obtained from numerical simulations together with the analytic curves. We can see that the growth rates obtained numerically agree very well with that calculated analytically. We also note that, in the parameter range plotted in Fig. 2 ($\alpha = 1$, $\kappa = 1$), the most unstable mode is $k_x \sim 0$, $k_y \sim 1$.

3. Simulation Results

The HW equations are solved in a double periodic slab domain with box size $(2L)^2 = (2\pi/\Delta k)^2$ where the lowest wavenumber $\Delta k = 0.15$. The equations are discretized on 256×256 grid points by the finite difference method. Arakawa's method is used for evaluation of the Poisson bracket[10]. Time stepping algorithm is the third order explicit linear multistep method[11].

Since we are focusing in this work on how the modification (9), (10) influences nonlinearly saturated states, we fix the parameters to $\kappa = 1$, $D_\zeta = 10^{-6}$, $\alpha = 1$, and $P_r = 1$, and compare the results obtained using the MHW model with those computed from the OHW model. For these parameters the system is unstable for most wavenumbers. During a typical evolution, initial small amplitude perturbations grow linearly until the nonlinear terms begin to dominate. Then the system arrives at a nonlinearly saturated state where the energy input Γ_n and output due to the resistivity Γ_α and the dissipations $D_{E,W}$ balance.

In Fig. 3, we contrast the zonally elongated structure of the saturated electrostatic potential computed from the MHW model with the strong isotropic vortices in that from the OHW model. Time evolution of the kinetic energy $E^{\mathrm{K}} = 1/2 \int |\nabla\varphi|^2 \mathrm{d}\boldsymbol{x}$, and its partition to the zonal and the non-zonal components are shown in Fig. 4. The saturated kinetic energy is not affected by the modification ($E^{\mathrm{K}} \sim 1$ for both cases). In the OHW model, the zonal flow grows in the linear phase, as well as the other modes, up to a few percent of the kinetic energy, and saturates. On the other hand,

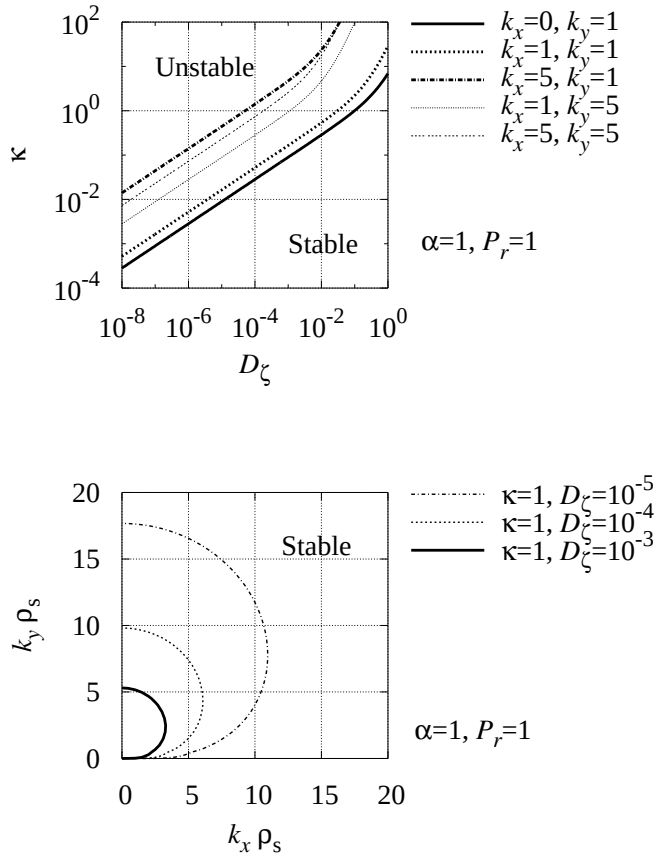

Fig. 1. Stability diagram of the MHW model. Left panel shows the stability thresholds in $D_\zeta - \kappa$ plane. The drift wave instability can be stabilized by strong dissipation. In the right panel, stability thresholds are plotted in $k_x - k_y$ plane. For certain parameters, only some low wavenumber modes are unstable.

in the MHW model the zonal kinetic energy continues to grow after the linear phase, and dominates the kinetic energy. The kinetic energy contained in other modes decreases to a few percent of the total kinetic energy. In the original 2D HW model, the resistive coupling term is retained for the zonal modes, the effect of which is to prevent development of zonal flows. But since the zonal modes do not carry parallel currents it is clearly unphysical

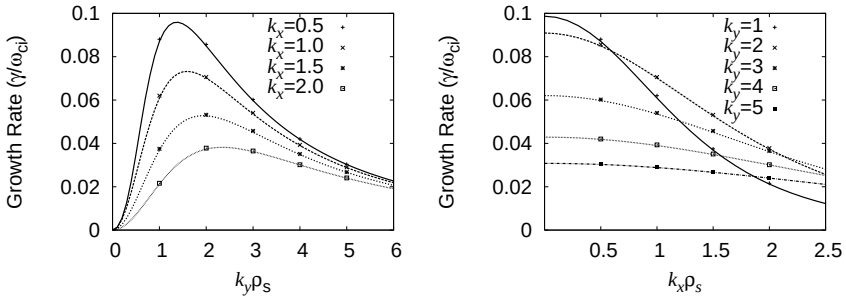

Fig. 2. Dispersion relation of the dissipationless MHW model. $\alpha = 1$, $\kappa = 1$.

to retain resistive action on them. Subtraction of the zonal components from the resistive coupling term is necessary to permit the generation of zonal flows.

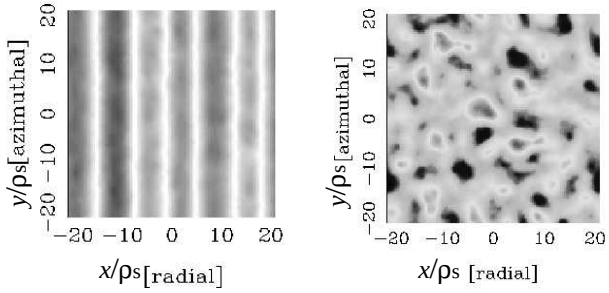

Fig. 3. Contour plots of saturated electrostatic potentials for the modified and the original HW models. Zonally elongated structure is clearly visible for MHW case.

The density flux in x direction Γ_n (transport across the magnetic field), together with the energy partition to the kinetic energy E^{K} and the potential energy $E^{\mathrm{P}} = 1/2 \int n^2 \mathrm{d}\boldsymbol{x}$, is plotted in Fig. 5. We observe that once the zonal flow is generated in the MHW model, the transport level is significantly suppressed. The transport suppression is mostly because the saturated potential energy (or amplitude of saturated density fluctuation) is reduced. The potential energy and the turbulence kinetic energy are converted into the zonal kinetic energy. By contrast the energy of the OHW model is almost equi-partitioned between the kinetic and potential energy.

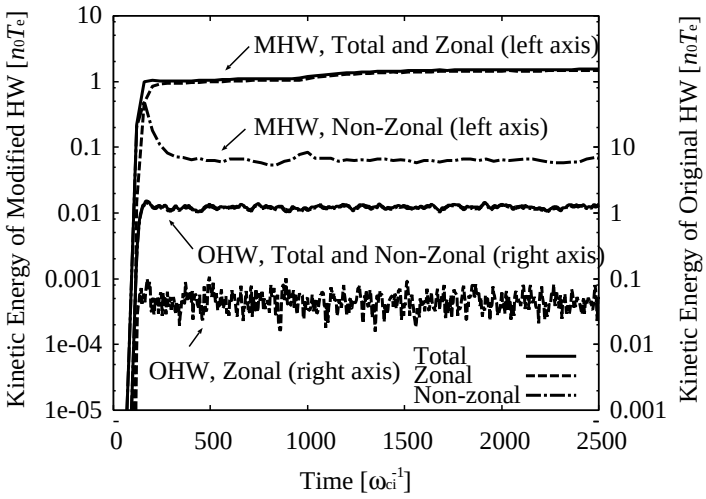

Fig. 4. Time evolution of the kinetic energy, and its partition to the zonal and the non-zonal components. In the modified HW model, the zonal mode contains most of kinetic energy, while non-zonal turbulence contains most of the kinetic energy in the original HW model.

The kinetic energy spectra averaged over the x or y direction for the MHW and the OHW models are shown in Fig. 6. The x (y) averaged kinetic energy spectra ($\mathcal{E}^{\rm K}_{x(y)}$) are defined from the Fourier amplitude of the kinetic energy $\mathcal{E}^{\rm K}$ by

$$\mathcal{E}^{\rm K}_y(k_x) = \frac{1}{K_y}\int_0^{K_y} \mathcal{E}^{\rm K}(k_x,k_y){\rm d}k_y, \tag{22}$$

$$\mathcal{E}^{\rm K}_x(k_y) = \frac{1}{K_x}\int_0^{K_x} \mathcal{E}^{\rm K}(k_x,k_y){\rm d}k_x, \tag{23}$$

where K_x, K_y are the highest wavenumbers. The spectra of the modified model again show strong anisotropic structure whereas there is no marked difference in the original HW model. In the modified model, potential energy stored in the background density is converted into turbulent kinetic energy through the drift wave instability at $k_y \sim 1$, $k_x = 0$ and then is distributed to smaller wavenumbers. The drift wave structure, which is elongated in the x direction, is break up into rather isotropic vortices after the nonlinear effect sets in, and those isotropic vortices merge in the y direction to produce the zonal flow. We can recognize this non-negligible inverse energy cascade in the y direction from a slight negative slope of $\mathcal{E}_x(k_y)$ spectrum in $k_y \lesssim 1$

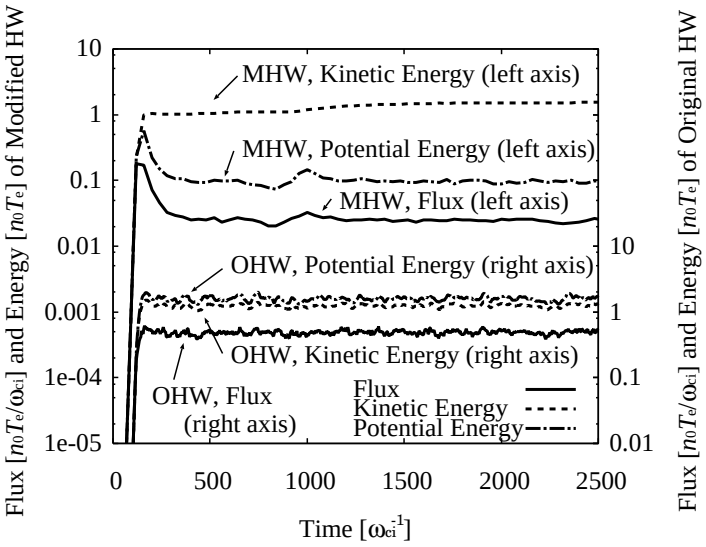

Fig. 5. Time evolutions of the radial density transport and the kinetic and the potential energies for the modified and the original HW models. Once zonal flow is generated in MHW model, the turbulent fluctuation level and transport are significantly reduced.

region. The y averaged spectrum $\mathcal{E}_x(k_y)$ shows the strong peak at the zonal wave number $k_x \sim 0.45$.

4. Conclusion

We have performed nonlinear simulations of the 2D HW model. As suggested recently[8], the electron response parallel to the background magnetic field must be treated carefully in the 2D model. The model should be modified to exclude the zonal ($k_y = 0$) contribution from the resistive coupling term. By comparing the numerical results of the modified and the unmodified original HW models, we have revealed that a remarkable zonal flow structure in the nonlinearly saturated state is only observed in the modified model. Thus, the modification is crucial to the generation of the zonal flow in this model. Time evolutions of the macroscopic quantities, such as the energies and fluxes show that, after the zonal flow is built up by turbulent interaction, the generated zonal flow significantly suppresses the turbulent fluctuation level and the cross-field density transport.

The build up of the zonal flow and resulting transport suppression indicate bifurcation structure of the system. If we increase a parameter (say,

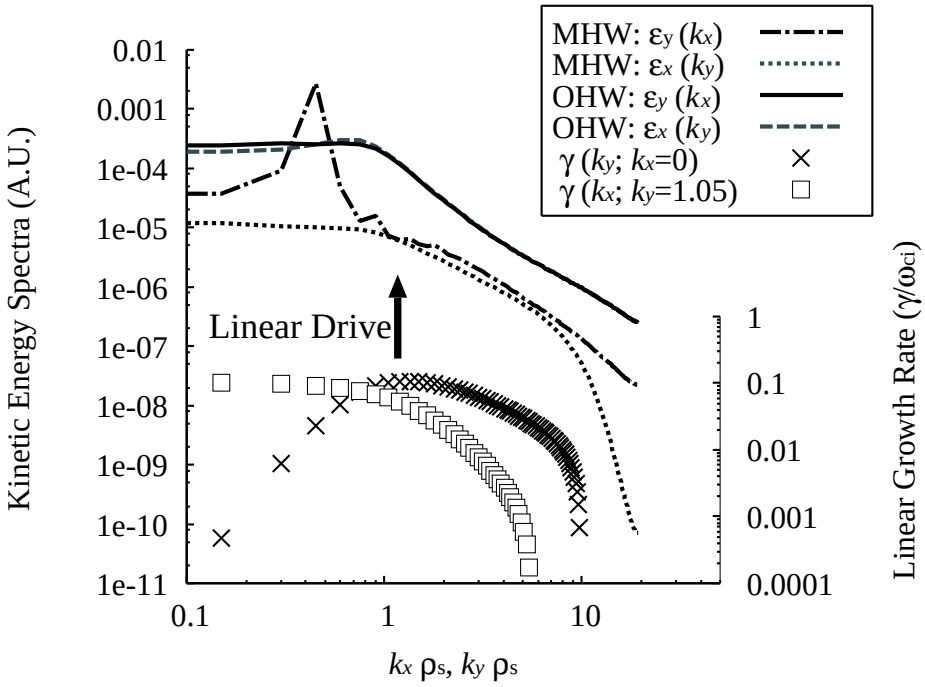

Fig. 6. The x and y averaged kinetic energy spectra for the MHW and the OHW models. The top two lines (solid line for $\mathcal{E}_y(k_x)$ and broken line for $\mathcal{E}_x(k_y)$) for the OHW model are almost overlapped indicating isotropy. The middle two lines (dot-dashed line for $\mathcal{E}_y(k_x)$ and dotted line for $\mathcal{E}_x(k_y)$) for MHW show highly anisotropic structure in low k region. The energy injected at $(k_x, k_y) = (0, 1)$ cascades inversely to the zonal mode of the wave number $(0.45, 0)$. The bottom two series of symbols show the linear growth rates of modes for reference.

strength of the linear drive term κ), the system may undergo sudden transition from a high transport to a low transport regime. The state shown in this paper can be a bifurcated state. A systematic parameter study and comparison with the low-dimensional dynamical model are possible next steps.

Acknowledgments

The simulation code used in this paper is provided by B.D. Scott. The authors would like to thank J.A. Krommes, F. Jenko and H.A. Dijkstra for fruitful discussions and comments during the Workshop on Turbulence and Coherent Structures. This work is supported by the Australian Research

Council.

References

1. P.H. Diamond *et al.*, *Phys. Rev. Lett.* **72**, 2565, (1994).
2. H. Sugama and W. Horton, *Plasma Phys. Control. Fusion* **37**, 345 (1995).
3. R. Ball, R.L. Dewar, and H. Sugama, *Phys. Rev. E* **66**, 066408 (2002); R. Ball, *Phys. Plasmas* **12**, 090904 (2005).
4. A. Hasegawa and M. Wakatani, *Phys. Rev. Lett.*, **50**, 682 (1983).
5. H. Sugama, M. Wakatani, and A. Hasegawa, *Phys. Fluids* **31**, 1601 (1988); A.E. Koniges, J.A. Crotinger, and P.H. Diamond, *Phys. Fluids B* **4**, 2785 (1992); S.J. Camargo, D. Biskamp, and B.D. Scott, *Phys. Plasmas* **2**, 48 (1995); G. Hu, J.A. Krommes, and J.C. Bowman, *Phys. Lett. A* **202**, 117 (1995).
6. A. Hasegawa and M. Wakatani, *Phys. Rev. Lett.* **59**, 1581 (1987).
7. A. Hasegawa and K. Mima, *Phys. Rev. Lett.* **39**, 205 (1977).
8. W. Dorland and G.W. Hammett, *Phys. Fluids B* **5**, 812 (1993); G.W. Hammett *et al.*, *Plasma Phys. Control. Fusion* **35**, 973 (1993).
9. R.H. Kraichnan and D. Montgomery, *Rep. Prog. Phys.* **43**, 547 (1980).
10. A. Arakawa, *J. Comput. Phys.* **1**, 119 (1966).
11. G.E. Karniadakis, M. Israeli, and S.A. Orszag, *J. Comput. Phys.* **97**, 414 (1991).